NISTIR 5421

STRENGTHENING METHODOLOGY FOR LIGHTLY REINFORCED CONCRETE FRAMES -II. RECOMMENDED CALCULATION TECHNIQUES FOR THE DESIGN OF INFILL WALLS

L.T. Phan
D.R. Todd
H.S. Lew

May 1994
Building and Fire Research Laboratory
National Institute of Standards and Technology
Gaithersburg, MD 20899

U.S. Department of Commerce
Ronald H. Brown, *Secretary*
Technology Administration
Mary L. Good, *Under Secretary for Technology*
National Institute of Standards and Technology
Arati Prabhakar, *Director*

ABSTRACT

Empirical equations were developed for estimations of ultimate lateral shear strength, story drift ratio at ultimate load, and ductility factor of existing lightly reinforced concrete frames (bare frames), existing monolithic shear walls, and reinforced concrete frames strengthened either by cast-in-place infilled walls or by single or multiple precast concrete panels. These equations were derived based on experimental results of many independently conducted test programs. Estimations of the ultimate shear stress, ultimate story drift ratio (story drift at ultimate load divided by story height), and ductility factor using the empirical equations compared favorably with the experimental results. The estimations confirm many observations made independently in individual test programs. The empirical expressions also provide "benchmark" values or ranges for these important parameters and thus provide a useful means for quick estimations of seismic capacity of bare, monolithic, and strengthened lightly reinforced concrete frames.

TABLE OF CONTENTS

1. INTRODUCTION 2
1.1 BACKGROUND 2
1.2 OBJECTIVES 3
1.3 SCOPE OF THIS REPORT 3

2. IDENTIFYING AND SELECTING EXISTING EXPERIMENTAL DATA 5
2.1 LITERATURE SEARCH: SEISMIC STRENGTHENING SCHEMES STUDIED 5
2.1.1 Infill Walls 5
2.1.2 Beam-Column Joint Upgrading 6
2.1.3 Steel Bracing, Frames, and Trusses 6
2.1.4 Column Strengthening 6
2.2 SELECTION OF EXPERIMENTAL DATA FOR MODEL DEVELOPMENT 6

3. IMPROVED HYSTERESIS FAILURE MODELS 8
3.1 DETERMINATION OF HYSTERESIS PARAMETERS THROUGH SYSTEM IDENTIFICATION 8
3.2 DEVELOPMENT AND VALIDATION OF HYSTERESIS FAILURE MODELS 8

4. EMPIRICAL FORMULAS FOR STRENGTH, DUCTILITY, AND STORY DRIFT RATIOS 12
4.1 DEVELOPMENT OF EMPIRICAL FORMULAS 12
4.2 VALIDATION OF EMPIRICAL FORMULAS FOR P_u/A_w, d_u/d_y, and μ_u 15

5. TOWARDS DESIGN GUIDELINES: SUMMARY OF OBSERVATIONS FROM EXPERIMENTAL PROGRAMS 20
5.1 GENERAL 20
5.2 POTENTIAL DESIGN GUIDELINES FOR STRENGTHENING WITH INFILL WALLS 20
5.2.1 Design of Infill Walls 20
5.2.2 Expected Lateral Strength, Story Drift Ratio, and Ductility Factor . 22
5.2.3 Other Design Considerations 23

6. SUMMARY, DISCUSSION AND FUTURE RESEARCH NEEDS 25
6.1 SUMMARY AND DISCUSSION 25
6.2 FUTURE RESEARCH NEEDS 26

7. REFERENCES 28

LIST OF TABLES

Table No. Page

1. Summary of Selected Infill Wall Tests 12

LIST OF FIGURES

Figure No.		Page
2.1	Typical CIP Infilled Frame	6
2.2	Exterior Beam_column Joint and Proposed Strengthening Scheme (After Beres et al., 1992)	7
2.3	Typical Steel Braced Frame	8
2.4	Typical "Jacketed" Column	9
2.5	Typical Aoyama's Test Specimen	11
2.6	Experimental Load-Displacement Plots of (a) Aoyama's Monolithic Specimen, and (b) Infilled Specimen	11
3.1	System Identification of Aoyama Test C2005-III	
	(a) Load-Deformation Characteristics	17
	(b) Absorbed Energy Histograms	17
3.2	System Identification of Ogata Test K3	
	(a) Load-Deformation Characteristics	18
	(b) Absorbed Energy Histograms	18
4.1	Load-Displacement of Aoyama's Specimen C2005-III (a), and Envelope Curve and It's Trilinear Approximation (b)	21
4.2	Predicted vs. Experimental Shear Strength of Frames	25
4.3	Error in Shear Strength Predictions	25
4.4	Predicted vs. Experimental Story Drift Ratio	26
4.5	Error in Story Drift Ratio Predictions	26
4.6	Predicted vs. Experimental Ductility Factor	27
4.7	Error in Ductility Factor Predictions	27

Chapter 1.

INTRODUCTION

1.1 BACKGROUND

A large percentage of the existing reinforced concrete (RC) buildings in the United States today were designed and constructed in accordance with past building codes which, if judged in light of today's knowledge of RC building performance in earthquakes, would be found inadequate. Significant advances in understanding of RC building behavior under earthquake loads occurred in the early 1970's. Modern seismic detailing requirements were first adopted into west coast building codes in 1976. Other parts of the country with significant seismic hazards adopted the changes somewhat later. Thus, virtually all RC buildings designed and constructed prior to the 1970's are today considered potentially vulnerable to earthquakes. Catastrophic failures that occurred in the 1971 San Fernando, 1985 Mexico City, and 1988 Armenia earthquakes, among others, illustrate the vulnerability of and potential for large loss of life in older or inadequately designed and built RC buildings.

Typical RC buildings generate large inertial forces when subjected to earthquake ground shaking due to their mass. The current detailing requirements for new buildings in regions of high seismicity make it possible for RC structures to develop the toughness and ductility necessary to inelastically resist these large forces without collapse. Buildings designed and constructed without these details are termed "lightly reinforced".

Little guidance is currently available on increasing the toughness and ductility of existing lightly reinforced concrete (LRC) buildings. However, the problem has been the focus of much research in recent years within the structural engineering community, in universities, Federal agencies, and the private sector. Many research projects on seismic strengthening of LRC buildings, both analytical and experimental, have been conducted. In an earlier phase of this project, a comprehensive literature survey [Phan, Todd, and Lew, 1993] revealed that a wide range of strengthening schemes have been proposed and experimentally tested. These schemes include techniques to strengthen frames, columns, and beam-column joints. Strengthening LRC frames through use of infill walls is found to be the technique for which the most experimental data is available.

One of the main limitations that has impeded development of guidelines for strengthening lightly reinforced concrete structures is the incomplete understanding of the seismic performance

of the strengthened structures up to failure. This has resulted in an inability to assess *quantitatively* the effectiveness of a strengthening technique. Further, this limitation has precluded comparisons between potential schemes, so optimization of design has been nearly impossible. A recent publication by the Building Seismic Safety Council (BSSC) for the Federal Emergency Management Agency (FEMA), "*NEHRP Handbook for Seismic Rehabilitation of Existing Buildings*" (1992), identified many techniques for strengthening various types of existing buildings. The document describes several strengthening schemes for LRC buildings and illustrates connections between the existing structure and the elements added for strengthening. While this document provides valuable insights into the practical aspects and the relative merits of the various retrofit techniques, still lacking is a method for quantitative assessment of the improvement in seismic performance of the strengthened structure.

Existing experimental data can be used to begin to fill this need. To date, many cyclic lateral load tests of LRC frame structures strengthened by different retrofit techniques have been conducted independently by researchers worldwide (Kahn, 1976; Sugano and Fujimura, 1980; Hayashi et al., 1980; Higashi et al., 1980; Oesterle et al., 1976 and 1979; Shiohara et al., 1984; Ogata and Kabeyasawa, 1984; Shah, 1989; Gaynor, 1988). These studies revealed, in a qualitative sense, the effectiveness of many commonly used strengthening schemes and the problems which might arise if these techniques are employed. Within each test program, conclusions have been drawn concerning the merits of the strengthening technique used. However, perhaps because experimental work is often cost inhibitive, none of the frame test programs had a broad enough scope to include all possible factors which might influence the seismic performance of the frame before and after being strengthened. Additional information can be extracted from these experiments through a systematic examination, based on statistical approaches, of all existing test programs.

This study focuses on utilizing the existing knowledge on the seismic performance of LRC frames obtained from various experimental programs to develop analytical techniques for evaluating quantitatively the effectiveness of common strengthening schemes. The analytical methods for performance evaluation and the experimental results will help in developing future design guidelines for seismic strengthening of lightly RC frame buildings.

1.2 OBJECTIVES

The overall objective of NIST's multi-year research program in this field is to use existing experimental research results to develop rehabilitation guidelines for seismic strengthening of LRC frame buildings. While researchers have tested numerous strengthening methods, including use of the infill walls, steel bracing, beam-column joint upgrading, and

column strengthening, a limited number of test results are available for some of the techniques. Therefore, this study will be limited to developing recommended design fuidelines for that strengthening technique for which sufficient data is available to lend credence to the results: the use of infill walls.

Most experimental test programs evaluate the behavior of single frame units or single bays to assess the potential effectiveness of various proposed strengthening schemes. Very little experimental data are available on the effectiveness of these schemes in complete structures, and almost no specific design guidance has been proposed. The intent of the NIST research effort is to make use of the available experimental data to develop valid analytical models which can assess the effectiveness of retrofit schemes in prototypical and actual buildings. Ultimately, design guidelines can be developed using the results of sufficient analytical studies.

Up to this point in the program, the focus has been on developing analytical tools for estimating both the hysteresis response and the critical parameters of existing and strengthened frames, such as ultimate shear strength, story drift ratio at ultimate load, and ductility. Once analytical techniques for performance evaluation of various strengthening schemes have been developed and validated, parametric studies can be performed. The results of the parametric studies can be utilized in developing the seismic rehabilitation guidelines.

1.3 SCOPE OF THIS REPORT

A report published in February 1993 (Phan et al., 1993) described earlier phases of this project: a literature search and the development of the first analytical tool, a set of hysteresis failure models for RC frames and frames with infills for use in nonlinear dynamic analysis programs such as IDARC or DRAIN-2D. Those phases are briefly summarized in this report in Chapters 2 and 3, respectively.

Chapter 4 of this report describes the development of a second analytical tool: a set of empirical equations for predicting the ultimate strength, ductility, and story drift of RC frames and frames with infills. Two types of infill additions, cast-in-place (CIP) walls and precast panels, are studied. The results of the experimental studies identified in the earlier phase of the project are systematically examined and utilized in developing analytical techniques for performance evaluation of

1) existing RC frames,
2) RC frames strengthened by CIP infill walls,

3) RC frames strengthened by precast infill panels, and
4) monolithic shear walls.

The two analytical tools are intended to reinforce each other. The hysteresis failure models allow for in-depth analysis of the existing and strengthened frames, including prediction of complete hysteresis performance of the structure at each stage of loading or deformation. The empirical formulas provide a simplified method for computing the critical parameters which are needed for evaluating the improved seismic performance of the strengthened structure. While either technique could be used to assess the efficacy of various strengthening schemes for a particular RC frame, because of the need for substantial computational capability, the hysteresis failure models lend themselves primarily to research uses.

Chapter 5 presents a summary of design-related observations from the experimental programs. These observations, along with the analytical tools, are expected to form the basis for design guidelines for seismic strengthening of RC frames through use of infill walls. The steps required to achieve that goal are outlined in Chapter 6.

Chapter 2

IDENTIFYING AND SELECTING EXISTING EXPERIMENTAL DATA

2.1 LITERATURE SEARCH: SEISMIC STRENGTHENING SCHEMES STUDIED

Most experimental test programs evaluate the behavior of single frame units or single bays to assess the potential effectiveness of various proposed strengthening schemes. Very little experimental data are available on the effectiveness of these schemes in complete structures, and almost no specific design guidance has been proposed. The intent of the NIST research effort is to make use of the available experimental data, or if necessary to conduct experimental studies, to develop valid analytical models which can assess the effectiveness of retrofit schemes in prototypical and actual buildings. Ultimately, design guidelines can be developed using the results of sufficient analytical studies. Detailed information on the earlier phases of this study can be found in Phan et al., 1993. This chapter gives a brief summary of the findings of the literature search that was used to identify existing experimental data appropriate for use in the project.

The literature review showed that the four most common strengthening techniques studied were:

1. **use of infill walls**, which involves filling the existing openings in RC frames with cast-in-place RC walls, precast concrete wall panels, or masonry;
2. **beam-column joint upgrading**, which aims to improve the lateral capacity of the joints by attaching external reinforcement (for example, bolted steel plates or angles) to the joint region;
3. **steel bracing**, which involves attaching steel sections, usually arranged into X-braces, K-braces, or V-braces, to the existing frames; and
4. **column strengthening**, which involves either increasing the size of the column by enclosing the existing column with a new layer of concrete and additional reinforcement, or connecting external steel plates to the existing column.

Beside these relatively common techniques, a number of unique strengthening techniques, designed specifically for a particular situation, have also been tested. The various techniques attempt to improve either the lateral strength capacity or the ductility of the existing structure, or the ability of the structure to dissipate the energy generated during an earthquake.

2.1.1 Infill Walls

The literature search showed that the use of infill walls has been studied more than any of the other seismic rehabiliation techniques for RC buildings. The majority of the test programs used scale models of one-bay, one-story lightly reinforced concrete frames (Aoyama et al., 1984 and 1986; Shiohara et al., 1984 and 1985; Kahn, 1976; Hayashi et al.,1980; Sugano and Fujimura, 1980; Higashi et al., 1980, 1981, and 1982; Corley et al., 1981; Oesterle et al., 1976 and 1979; Ogata and Kabeyasawa, 1984; Gaynor, 1988, and Shah, 1989). In general, infill walls that have been experimentally tested have been typically constructed using:

- cast-in-place (CIP) concrete, connected to the existing construction with epoxied or wedge anchor dowels, and/or shear keys;
- precast concrete, using either single or multiple panels, connected by welding to new steel anchors in the original construction;
- masonry, either brick or concrete block;
- steel panels, connected by welding to new anchors in the existing structure; or
- pneumatically applied concrete (shotcrete).

Rigid infill walls act primarily as shear walls. Because of the relative rigidity of the infilled bays, the demand on the existing frame is substantially reduced. This is especially true for buildings with rigid diaphragms. Frames with less rigid infill, such as unreinforced masonry, often used to form exterior walls in original construction, will behave like braced frames with the infill acting as a compression strut.

Tests of solid CIP concrete infill walls demonstrate that the strength and stiffness of the retrofit structure approaches that of a monolithically cast wall. Tests of frames infilled with precast concrete panels show that with this technique the retrofit frame attains slightly less than half the strength of the monolithic wall. Typical configuration of an infilled frame is shown in Figure 2.1

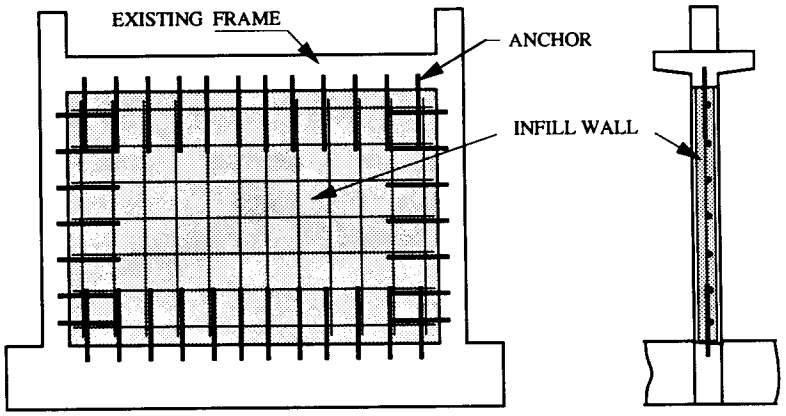

Figure 2.1 Typical CIP Infilled Frame

2.1.2 Beam-Column Joint Upgrading

In theory, improving the strength and/or toughness of the beam-column joints in a concrete frame will improve the overall ductility of the building. Although many experimental studies of the behavior of typical interior and exterior joints under cyclic loads have been conducted to date (Kaku et al., 1985; Kanada et al., 1985; Durrani and Wight, 1982; Ruitong and Park, 1987; Pessiki et al., 1990; Ehsani and Alameddine, 1989; Sugano et al., 1990; Gavrilovic et al., 1980; Kitayama et al., 1985 and 1986; Beckingsale et al., 1980; Choudhuri et al., 1992), there has been very little experimental testing of joint strengthening techniques (Alcocer and Jirsa, 1990). In an attempt to partially fill this gap, NIST, in an earlier phase of this multi-year existing concrete buildings research program, carried out a joint study at Cornell University to design, construct, and test several joint strengthening techniques (Beres et al., 1992). Testing showed significant improvements in the behavior of the strengthened specimens: cover was protected, and peak strength, initial stiffness, and energy dissipation capacity were increased. Figure 2.2 shows the configuration and proposed strengthening scheme for an exterior beam-column joint tested by Beres et al. (1992).

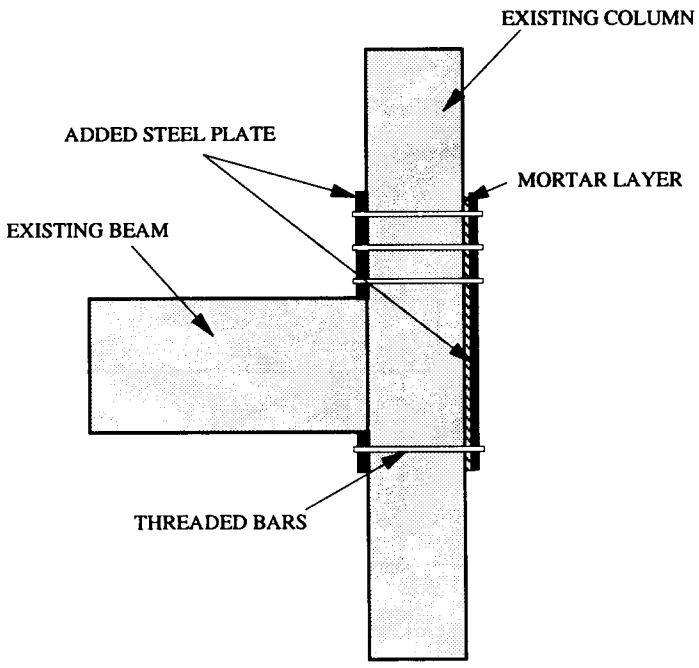

Figure 2.2 Exterior Beam-Column Joint and Proposed Strengthening Scheme (After Beres et al., 1992)

2.1.3 Steel Bracing, Frames, and Trusses

Steel braces, steel frames, or steel trusses can be concentrically or eccentrically added to existing RC frame buildings, through use of mechanical connectors, to supplement the existing lateral force resisting system. In concentrically braced frames, steel braces are inserted in the frame opening to enhance the ductility and strength of the existing concrete frame. In eccentrically braced frames, complete steel structural systems, which are continuous through the floor slabs and attached to the building exterior, can be designed to essentially replace the existing lateral force resisting system. These schemes typically require the addition of collectors (structural tees and steel channels), usually attached to beams and columns with anchor bolts embedded in the frame, to transfer the load from the existing frame to the brace members. In general, steel bracing has been found to provide moderate increases in lateral load capacity and more significant increases in ductility to the existing RC frames.

A wide range of bracing configurations, including Diagonal bracing, in-plane compression X-bracing, in-plane tension X-bracing, K-bracing, V- and inverted V-bracing, can be designed to strengthen RC frames. Most of these configurations have been experimentally tested (Sugano and Fujimura, 1980; Higashi et al., 1981 and 1982; Jones and Jirsa, 1986; Bush et al., 1986; Goel and Lee, 1990). Some have also been actually employed to strengthen existing buildings (Kawamata and Ohnuma, 1980). Regardless of the type of bracing configuration, the steel bracing technique has an inherent disadvantage. That is, since the braces are connected to the existing frame at beam/column ends, the forces resisted by the braces will be transfered back to the concrete beams and columns in the form of axial forces (both in compression and in tension, as the frame undergoes cyclic lateral load). While the addition of compressive forces to the designed gravity load in the beam and column may be tolerated, the resulting tensile forces may be cause for concern, especially for column, since they were designed primarily for gravity load. Figure 2.3 shows a typical RC frame strengthened by compression X-bracing technique.

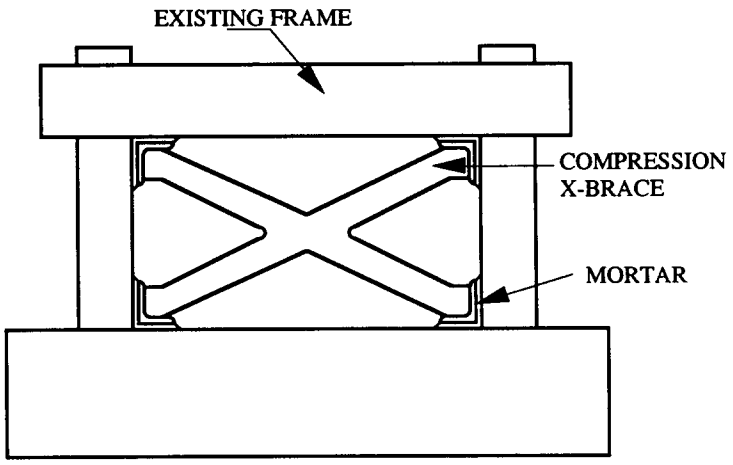

Figure 2.3 Typical Steel Braced Frame

2.1.4 Column Strengthening

Most column strengthening techniques add transverse reinforcement in an attempt to improve ductility. Column strengthening techniques that have been experimentally studied include:

- encasing the column in steel plates or pipes and filling the gap with grout;
- attaching tightly fitted steel bands or straps around the column; and
- enlarging the column with additional reinforced concrete, using either welded wire fabric or closely spaced ties for transverse reinforcement, and either pneumatically applied or cast-in-place (CIP) concrete.

These techniques are often generically termed "jacketing". Where the flexural capacity of the column is adequate, gaps are left at top and bottom of the jacketing to avoid increasing the flexural capacity and related induced shear forces. Testing programs by Hayashi et al., 1980; Nene, 1985; Bett et al., 1985; Choudhuri et al., 1992; Kahn, 1980; and Roach and Jirsa, 1986, have verified the ability of these techniques to strengthen and stiffen columns. Jacketing columns creates many of the same construction and occupant dislocation problems as does infilling frames. However, permanent disruption of traffic flow, loss of window space, and other major changes in building function will not occur. Figure 2.4 shows a typical cross section of a "jacketed" column.

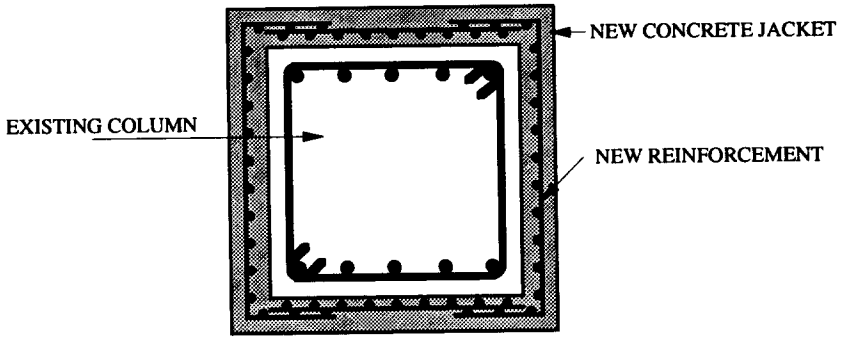

Figure 2.4 Typical "Jacketed" Column

2.2 SELECTION OF EXPERIMENTAL DATA FOR MODEL DEVELOPMENT

Because of the availability of experimental data, strengthening through use of infill walls was selected for further study. Descriptions of the experimental studies and the characterisitics of the test specimens are listed in Table 1.

Fifty-four specimens were selected for use in developing the hysteresis failure models and empirical formulas for ultimate shear strength P_u, story drift ratio at ultimate load d_u/H_c, and ductility factor μ_u. These were from experiments conducted by Aoyama et al., 1984 and 1986; Shiohara et al., 1984 and 1985; Kahn, 1976; Hayashi et al., 1980; Sugano et al., 1980; Higashi et al., 1980; Corley et al., 1976, 1979, and 1981; Ogata et al., 1984; and Gaynor, 1988. The specimens consisted of five bare frames, twenty-one monolithic wall-frame constructions, twenty-one frames strengthened by CIP infill wall, and eight frames strengthened by precast concrete panels. In most cases, the frames were designed to have reinforcement details that are typical of LRC construction - i.e., low longitudinal reinforcement ratio for columns, little or no transverse reinforcement within the beam-column joint regions, and large spacing between column transverse reinforcement which results in little confinement of the concrete core. The ranges of some typical parameters of the specimens included in this study are as follows:

- Flexural Reinforcement ratio of column (%) : 0.71 to 5.35
- Shear Reinforcement ratio of column (%) : 0.07 to 1.92
- Ratio of beam clear span/column height : 0.40 to 1.90
- Frame concrete compressive strength (MPa) : 17.9 to 53.8
- Column axial stress (MPa) : 0.0 to 3.75

The dimensions, reinforcement details, and scale factors of the specimens were selected independently by the various researchers who conducted the experiments. The specimens used in this study were selected using the following criteria:

- The test specimens are one-bay one-story frames.
- The loading program is quasi-static reversed cyclic.
- Strengthening is accomplished by reinforced concrete infill wall.
- Reinforcement details in the existing frame are typical of LRC construction.

The use of one-bay one-story frame tests limits the number of variables that need to be considered and permits direct comparison of test results between the various test programs. It also allows the most efficient utilization of existing test data relevant to seismic strengthening since the majority of seismic strengthening tests on RC frames are one-bay one-story. Further,

the hysteresis failure models developed for RC frames based on one-bay one-story tests are versatile and may easily be incorporated into computer programs such as IDARC for use in the analysis of RC structures strengthened using various schemes.

Experimental tests which did not meet the criteria indicated above were not utilized in developing the hysteresis failure models and empirical formulas. However, the results of those tests will provide useful data for validating this and future analytical developments. In general, all of the selected experimental results were in the form of cyclic lateral load-lateral displacement plots. The analog data were digitized and a digital database was created for this project. Complete set of load-displacement plots may be found in Phan et al. (1993). A typical test specimen and load-displacement plots are shown below.

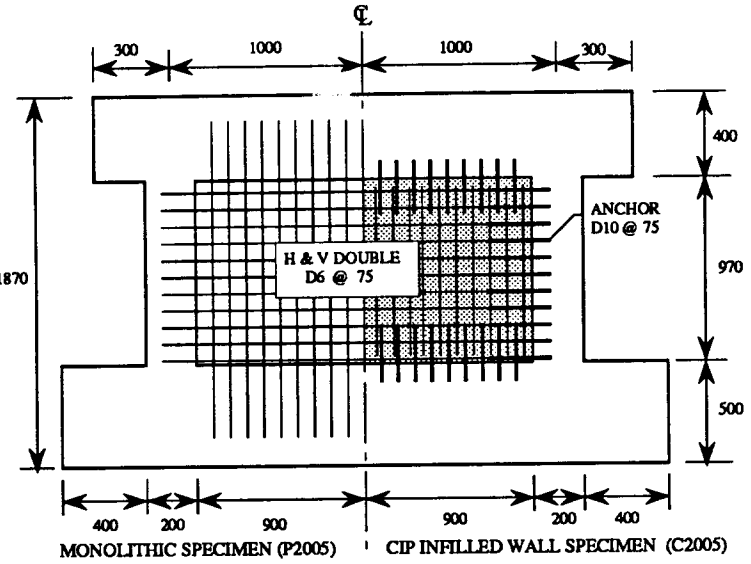

Figure 2.5 Typical Aoyama's Test Specimen

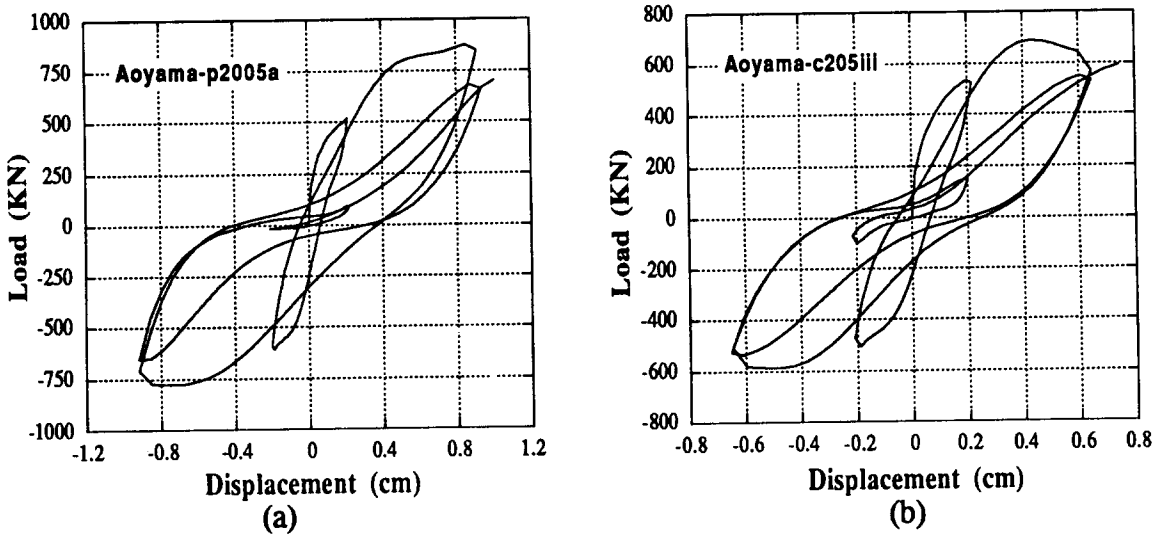

Figure 2.6 Experimental Load-Displacement Plots of (a) Aoyama's Monolithic Specimen, and (b) Infilled Specimen

Table 1. Summary of Selected Infill Wall Tests

Test	Column bxD (cm)	Column A_g (cm^2)	Concrete f'c (MPa) Frame	Concrete f'c (MPa) Wall	P_x/A_{cg} (MPa)	L_b/H_c	Construction and Anchor Type	Max. Load P_u (KN)	Max. Shear Strength P_u/A_w (MPa)	Story Drift at Ultimate Load $100x(d_u/H_c)(\%)$	Ductility Factor $\mu_u=d_u/d_y$
AOYAMA:											
C2005-I	20x20	5.08	23.1	20.1	2.94	1.86	CIP Infill/Epoxy	749.1	2.75	0.58	5.6
C2005-II	20x20	5.08	23.1	20.1	2.94	1.86	CIP Infill/Epoxy	722.4	2.64	0.57	11.0
C2005-III	20x20	5.08	22.2	21.6	2.94	1.86	CIP Infill/Epoxy	674.4	2.46	0.48	6.6
C2015-A	20x20	15.2	21.9	14.7	2.94	1.86	CIP Infill/Epoxy	1033.8	3.71	0.71	17.3
C2015-B	20x20	15.2	19.4	14.7	2.94	1.86	CIP Infill/Epoxy	998.2	3.66	0.70	8.5
C2015-C	20x20	15.2	39.5	38.6	2.94	1.86	CIP Infill/Epoxy	1420.8	2.22	1.68	12.2
P2005	20x20	5.08	21.6	21.6	2.94	1.86	Monolithic	870.1	3.18	0.82	11.4
P2015	20x20	15.2	38.6	38.6	2.94	1.86	Monolithic	1522.2	5.36	0.76	10.6
C4015	20x40	15.2	22.9	29.1	1.47	1.65	CIP Infill/Epoxy	1121.0	3.25	0.72	11.7
P4015	20x40	15.2	29.1	29.1	1.47	1.65	Monolithic	1467.9	4.22	0.71	9.9
M2005	20x20	5.08	29.5	28.1	2.94	1.86	CIP Infill/Wedge	685.0	2.48	0.62	12.0
CH2015	20x20	15.2	28.3	21.8	2.94	1.86	Expansive CIP Infill/Epoxy	1085.4	4.04	0.68	9.4
CH2018	20x20	18.1	25.6	21.8	2.94	1.86	Expansive CIP Infill/Epoxy	1058.7	3.94	0.81	7.9
OLU2015	20x20	15.2	21.9	17.7	2.94	1.86	Expansive CIP w/opening/Epoxy	693.9	2.53	0.76	4.6
KAHN:											
SP1	15x15	8.0	34.4	34.4	0.0	1.63	Monolithic	666.3	2.38	1.39	4.8
SP2	15x15	8.0	31.1	-----	0.0	1.63	Bare Frame	41.8	0.71	3.70	8.8
SP3	15x15	8.0	24.7	19.4	0.0	1.63	CIP Infill/Epoxy	502.6	1.92	0.93	10.8
SP4	15x15	8.0	24.3	20.1	0.0	1.63	Multiple Precast Panel/Welded Connectors	271.3	1.03	1.97	10.5

Test	Column bxD (cm)	A_g (cm^2)	Concrete f'c (MPa) Frame	Wall	P_x/A_{cg} (MPa)	L_b/H_c	Construction and Anchor Type	Max. Load P_u (KN)	Max. Shear Strength P_u/A_w (MPa)	Story Drift at Ultimate Load $100x(d_u/H_c)(\%)$	Ductility Factor $\mu_u=d_u/d_y$
HAYASHI:											
W-1	20x20	5.07	17.9	----	2.94	1.78	Bare Frame	99.6	1.27	1.87	9.3
W-2	20x20	5.07	17.9	17.9	2.94	1.78	Monolithic	689.5	3.34	1.17	11.7
W-4	20x20	5.07	17.9	26.7	2.94	1.78	CIP Infill/Wedge	489.3	2.34	0.82	18.5
W-5	20x20	5.07	18.1	30.0	2.94	1.78	CIP Infill/Wedge	427.0	2.02	0.60	6.0
W-6	20x20	5.07	18.1	30.0	2.94	1.78	CIP Infill/Wedge	489.3	2.27	0.44	13.3
SUGANO:											
F	20x20	5.16	23.5*	----	3.06	1.88	Bare Frame	114.8	1.42	1.75	23.3
W-80S	20x20	5.16	23.5*	37.3*	3.06	1.88	Monolithic	642.3	3.11	0.39	31.0
W-40S	20x20	5.16	23.5*	37.3*	3.06	1.88	Monolithic	470.6	3.15	0.48	34.1
W-40W	20x20	5.16	23.5*	37.3*	3.06	1.88	Monolithic w/thickened wall	562.3	3.74	0.33	26.0
W-HA	20x20	5.16	23.5*	37.3*	3.06	1.88	CIP Infill/Wedge	631.6	3.16	0.70	43.5
W-BL	20x20	5.16	23.5*	29.4*	3.06	1.88	Precast block Infill	402.1	1.70	0.86	68.0
W-CO	20x20	5.16	23.5*	37.3*	3.06	1.88	CIP Infill/ Mortar shear keys	562.3	2.66	0.44	35.0
CORLEY:											
B5	31x31	34.1	45.3	45.3	0.0	0.43	Monolithic	691.3	1.80	2.61	23.5
B6	31x31	34.1	21.8	21.8	2.93	0.43	Monolithic	771.3	2.02	1.32	9.48
B7	31x31	34.1	49.3	49.3	3.76	0.43	Monolithic	923.5	2.38	2.21	41.0
B8	31x31	34.1	41.9	41.9	3.76	0.43	Monolithic	960.8	2.40	2.08	15.2
B9	31x31	34.1	44.1	44.1	3.76	0.43	Monolithic	886.1	2.37	2.59	17.3
B11	31x31	34.1	53.8	53.8	0.0	0.43	Monolithic	659.2	1.80	2.31	13.1

Test	Column bxD (cm)	A_g (cm^2)	Concrete f'c (MPa) Frame	Wall	P_x/A_{cg} (MPa)	L_b/H_c	Construction and Anchor Type	Max. Load P_u (KN)	Max. Shear Strength P_u/A_w (MPa)	Story Drift at Ultimate Load $100x(d_u/H_c)(\%)$	Ductility Factor $\mu_u=d_u/d_y$
HIGASHI:											
1-F1	20x20	5.16	17.3	----	2.94	1.78	Bare Frame	95.2	0.50	1.38	4.9
2-PW	20x20	5.16	17.3	21.5	2.94	1.78	CIP Infill/Wedge	355.9	1.61	0.60	3.60
5-F2	20x20	5.16	20.6	----	2.94	1.78	Bare Frame	98.8	1.25	2.08	7.8
13-FW	20x20	5.16	20.6	20.6	2.94	1.78	Monolithic	516.0	2.30	0.71	5.8
4-C3C	20x20	5.16	17.3	23.7	2.94	1.78	Precast Panels	409.2	1.86	1.00	7.5
6-C2A	20x20	5.16	21.5	22.4	2.94	1.78	Precast Panels w/Center Opening	139.7	0.67	1.97	44.3
7-C2B	20x20	5.16	21.5	22.4	2.94	1.78	Precast Panels w/Side Opening	129.0	0.62	1.98	19.7
9-C40	20x20	5.16	21.5	22.4	2.94	1.78	Precast Panels	142.3	0.71	1.98	29.7
3-C3	20x20	5.16	17.3	23.7	2.94	1.78	Precast Panels	293.6	1.45	1.74	12.0
8-C4	20x20	5.16	21.5	22.4	2.94	1.78	Precast Panels	355.9	1.72	0.71	7.1
OGATA:											
K1	20x20	2.8	19.2	19.2	1.88	1.07	Monolithic	400.3	1.83	0.78	7.3
K2	20x20	5.7	19.2	19.2	1.88	1.07	Monolithic	435.9	1.97	0.93	6.6
K3	20x20	8.6	19.2	19.2	1.88	1.07	Monolithic	491.1	2.18	0.93	7.3
K4	20x20	5.7	20.8	20.8	1.88	1.07	Monolithic	462.6	2.11	0.94	10.4
K5	20x20	5.7	20.8	20.8	1.88	1.07	Monolithic	532.9	2.50	0.87	4.8
K6	20x20	8.6	20.8	20.8	1.88	1.07	Monolithic	661.0	2.63	0.84	5.5
GAYNOR:											
F	31x31	20.6	28.6	23.3	0.0	1.76	Shotcrete Infill	1052.4	1.42	0.32	28.1
W	31x31	20.6	38.4	21.4	0.0	1.76	Shotcrete Infill w/Window Opening	764.2	1.10	0.49	36.3
D	31x31	20.6	33.0	22.6	0.0	1.76	Shotcrete Infill w/Door Opening	876.3	1.18	0.51	18.3

Chapter 3

IMPROVED HYSTERESIS FAILURE MODELS

3.1 GENERAL

Hysteresis failure models, which characterize the load-deformation histories of existing and strengthened RC frames up to failure, were developed and incorporated into the platform program IDARC for use in nonlinear dynamic analysis of the strengthened frames. In this context, hysteresis failure models are represented by three hysteresis parameters: the stiffness degradation parameter α, the strength deterioration parameter β, and the pinching parameter γ. More detailed discriptions of α, β, and γ may be found in Park et al., 1987; Kunnath and Reinhorn, 1989; and Phan et al., 1993. In the simplest terms, the parameter α governs the reduction in stiffness of reinforced concrete members as they undergo reversed cyclic loading in the inelastic range. The parameter β governs the rate of strength reduction, and is generally a function of cumulative absorbed energy and maximum displacement in each loading cycle. The parameter γ determines the level of "pinching" or contriction of the hysteresis behavior of the reinforced concrete members. The procedure used for the development of the three-parameter hysteresis models in this study involved the following two main tasks:

1. Determine the values for three parameters α, β, and γ which best fit the experimental hysteresis loop of each of the fifty four tests selected above using the system identification technique (Kunnath et al., 1989 and Yeh, 1987). The corresponding fifty four sets of α, β, γ, so determined are from here on referred to as the estimated parameters α, β, γ. This task is briefly described in section 3.2.

2. Based on the fifty four sets of estimated parameters α, β, and γ, perform multiple-variable regression to obtain mathematical expressions for α, β, and γ in terms of the physical properties of the selected test specimens. These mathematical expressions, referred to in this study as the hysteresis failure models, are then used to predict the three parameters for the analysis of bare frames, infilled frames, and monolithic wall-frame constructions. This task is briefly described in section 3.3

3.2 DETERMINATION OF HYSTERESIS PARAMETERS THROUGH SYSTEM IDENTIFICATION

The concept of identifying or estimating hysteresis parameters of concrete structures subjected to cyclic loading using actual test results has been tried by many researchers. The purpose is to derive a set of parameters which may be used to simulate as closely as possible the hysteresis behavior observed from experiment. Earlier research included the work by Yeh (1987) at SUNY/Buffalo which utilized nonlinear search algorithms and optimization techniques to obtain the best possible set of hysteresis parameters based on the actual test results. Later modification of the optimization techniques used by Yeh (1987) were performed at NIST by Stone and Taylor (1992). The result is a graphics-based system identification package, called NIDENT 3.0. Principally, the system identification procedure performs a three dimensional trial and error search for a set of initial values of α, β, γ such that the cumulative error between the predicted and experimentally observed hysteretic energy is minimized. NIDENT 3.0 displays the hysteresis response corresponding to the initial parameters together with the experimentally-observed response. The users are then allowed to interactively adjust the values of α, β, and γ while continuously monitoring the fit between the predicted and the experimentally-observed responses in real time until a satisfactory match between the responses is observed. At any time during the fitting process, a check of cumulative error, in terms of the absorbed hysteretic energy, between the latest prediction and the experimentally-observed response can be performed. Generally, a reasonable visual match of the hysteretic responses and an absorbed energy cumulative error of within a few percent is considered satisfactory. The values of α, β, and γ so determined constitute the identified hysteresis parameters of the corresponding experiment. A more detailed discussion concerning NIDENT 3.0 is given in Stone and Taylor (1992).

Examples of the match between the system identified and measured hysteresis responses of two test specimens, Aoyama's infilled frame specimen C2005-III and Ogata's monolithic wall-frame specimen K3, are shown in Figures 3.1 and 3.2. The dashed lines represents the experimental results and the solid lines are the predicted (system identified) hysteresis response corresponding to the estimated hysteresis parameters α, β, γ, obtained from system identification. Also plotted are histograms of the measured and predicted absorbed energy for the test specimens. As can be seen in these figures, the three parameters α, β, γ, identified for the test specimen were able to characterize reasonably well the load-deformation hysteresis behavior of the test specimens. The absorbed energy of the specimens on a per cycle basis, calculated for the system identified load-deformation response, also compared well with the absorbed energy calculated from experimental load-deformation response.

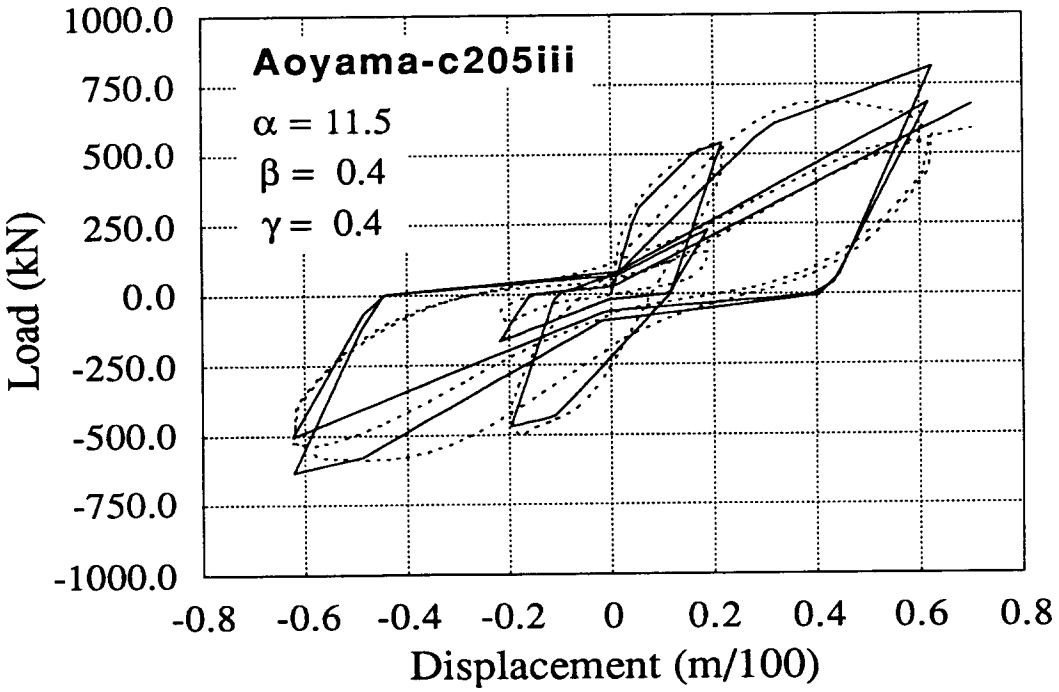

(a)

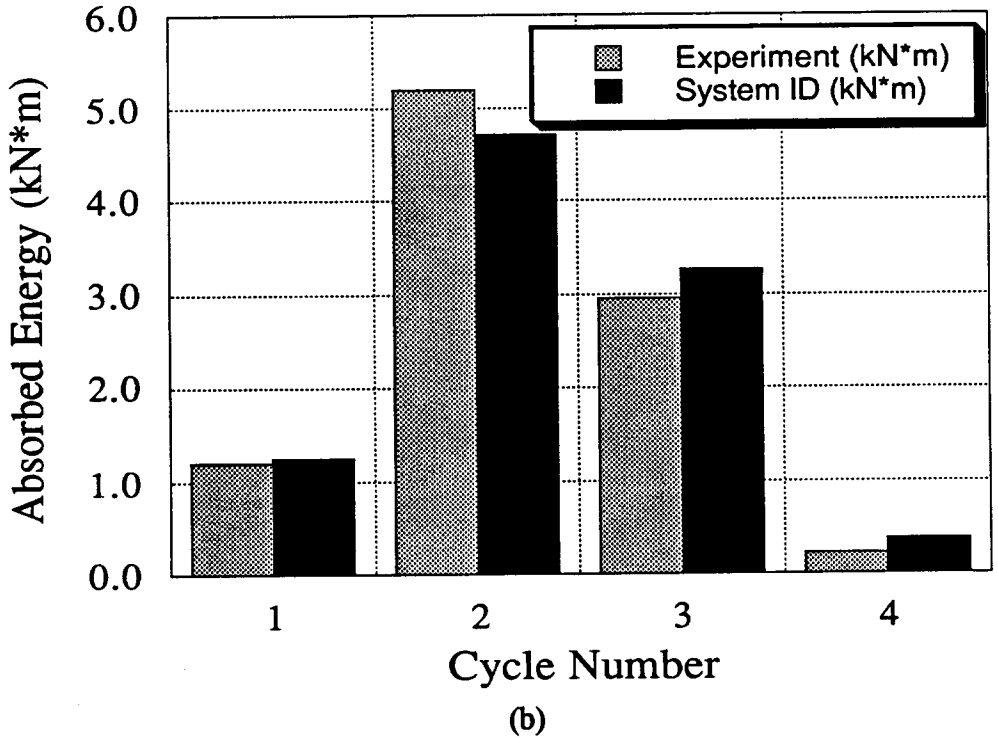

(b)

Figure 3.1 System Identification of Aoyama Test C2005-III

(a) Load-Deformation Characteristics

(b) Absorbed Energy Histograms

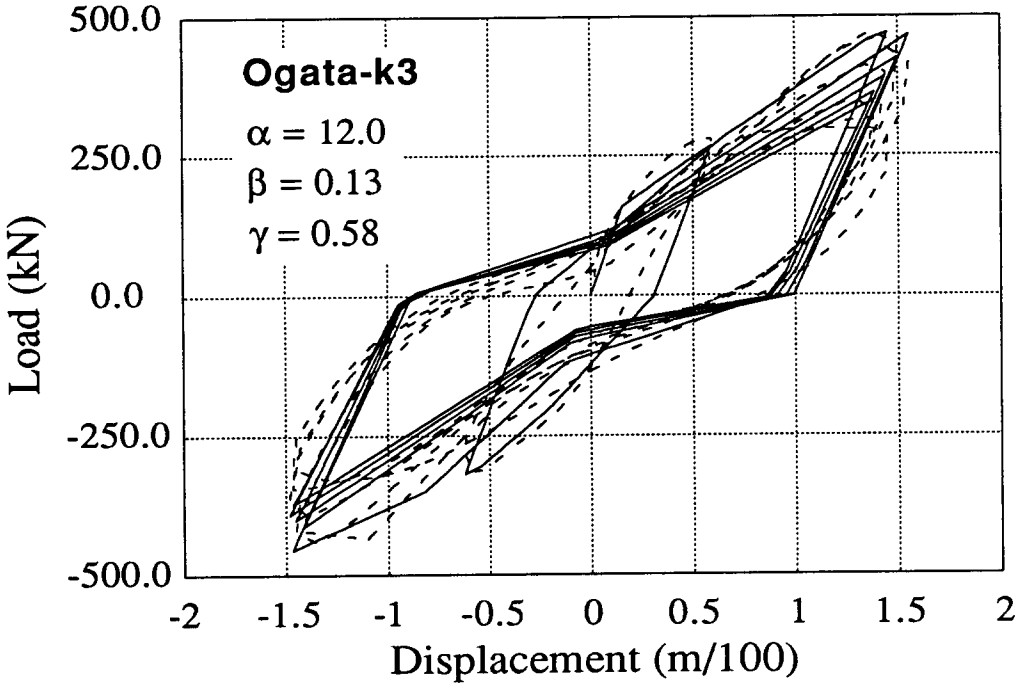

(a)

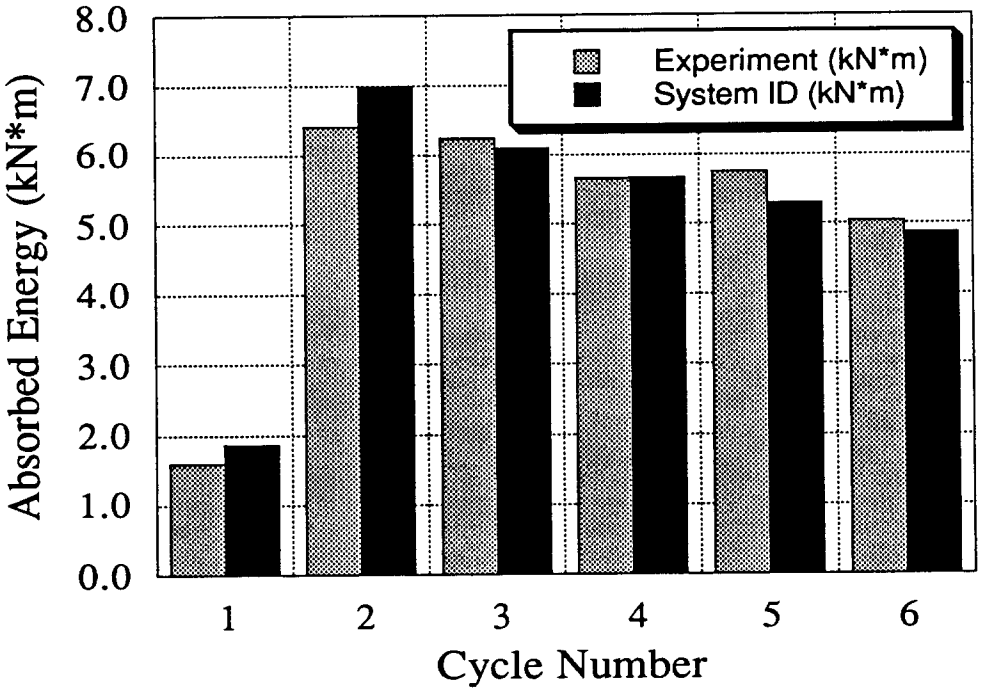

(b)

Figure 3.2 System Identification of Ogata Test K3

(a) Load-Deformation Characteristics

(b) Absorbed Energy Histograms

3.3 DEVELOPMENT AND VALIDATION OF HYSTERESIS FAILURE MODELS

With a sufficient number of sets of hysteresis parameters (α, β, γ) for existing and strengthened RC frames - i.e. sufficient number of experimental data - the hysteresis parameters can then be expressed as functions of the physical characteristics (such as geometric dimensions, material properties, and reinforcement patterns) of structural systems being examined by statistical analysis. These expressions, referred to hereafter as hysteresis failure models, allow the calculation of α, β, and γ, which characterize the hysteresis behavior of the RC frames, through use of the frames' geometric and material properties. The hysteresis failure models so developed can be incorporated into platform computer programs such as IDARC or DRAIN-2D for analyses of existing and strengthened RC frames.

Hysteresis failure models were developed for 1) existing RC frames, 2) frames with CIP infill walls, 3) frames infilled with precast panels, and 4) monolithic wall-frame construction. The mathematical expressions for these models can be found in Phan et al., 1993. The models were then used to derive values for α, β, and γ for each of the fifty-four test specimens. The predicted values were compared to the values selected using the system-identification technique, and were found to match well.

The models were then used to calculate α, β, and γ for a one-story one-bay infilled frame and for a three-story one-bay infilled frame. Load-deformation characteristics, per-cycle absorbed energy, and ultimate load capacity predicted by IDARC using the calculated α, β, and γ were compared to the behavior of the experimentally tested models. Using the hysteresis failure models, IDARC provided a substantially improved prediction of frame behavior compared to that obtained using default IDARC hysteresis values. The procedure used to develop and validate the hysteresis failure models is described in more detail in Phan et al., 1993.

Chapter 4

EMPIRICAL FORMULAS FOR STRENGTH, DUCTILITY, AND STORY DRIFT RATIOS

4.1 DEVELOPMENT OF EMPIRICAL FORMULAS

Using the same set of experimental data used in developing the hysteresis failure models, empirical formulas for quick estimation of parameters critical for retrofit design were developed. The parameters for which predictive equations were developed are:

- ultimate shear strength P_u/A_w,
- story drift ratio at ultimate load, d_u/h_c (ratio of story displacement at ultimate load d_u and story height h_c), and
- ductility factor μ_u (defined as the ratio between displacement at ultimate load d_u and displacement at first yield d_y, d_u/d_y).

The technique used in developing the empirical formulas is similar to that used in developing the hysteresis failure models. First, from the experimental hysteresis response of an experiment, the envelope of the load-deformation response was developed. Then, by approximating that load-deformation envelope as a trilinear response, the information of interest (experimental lateral load capacity P_u, story drift ratio d_u/H_c, and ductility factor μ_u) for that specimen were extracted.

Figure 4.1 shows a typical envelope curve from a specimen tested by Aoyama et al. (1984 and 1986) and the trilinear approximation of the hysteresis response. The maximum load attained at the end of the first linear branch is considered the load at which yielding of the reinforcement begins and is denoted as P_y. The corresponding displacement is yield displacement and is denoted d_y (story drift at yield). The maximum attainable load is denoted as P_u, and the corresponding displacement, d_u (story drift at ultimate). Statistical analysis was then performed to relate P_u, d_u/H_c, and μ_u to the geometric and material properties of the RC frames and infills. These relations constitute the empirical formulas for lateral strength P_u/A_w, story drift ratio d_u/h_c, and ductility factor μ_u, as shown in equations 1 to 3.

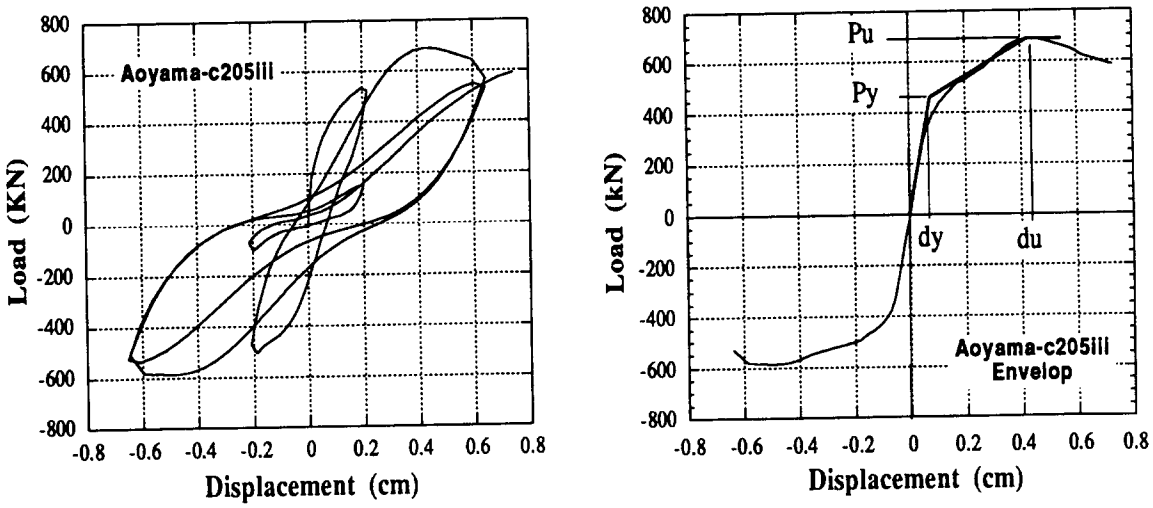

(a) (b)

Figure 4.1 Load-Displacement of Aoyama's Specimen C2005-III (a), Envelope Curve and It's Trilinear Approximation (b)

$$\frac{P_u}{A_w} = -1.454 + 0.237(\rho_{tb}) + 0.343(\rho_{bb}) + 3.612\left(\frac{P_{xc}}{A_{cg}f_{cf}}\right) + 23.46\times10^{-6}\left(\frac{12E_{cf}I_c}{h_c^3}\right) - 16.454(t_w) - 6.924(A_o) + 0.343(\rho_c) + 1.62\times10^{-3}(f_{ya}) + 2.16(A_{ca}f_{ya}) + 7732(A_{stb}) - 19.86(A_{stb}f_{ystb}) + 8.9(S_{sbb}) + 3.67\times10^{-3}(f_{yw})$$

$$100\left(\frac{d_u}{h_c}\right) = 1.36 + 17.66(A_{tb}) - 3.63(\rho_{vtb}) - 2.4(A_{bb}) + 0.05(f_{cf}) + 19.34(t_w) - 2.445(I_w) - 7.53\times10^{-3}(f_{yw}) + 0.77\left(\frac{L_{tb}}{n.L_{pe}}\right) - 2.5(S_{atb}) - 3.84\times10^{-5}(t_w L_{tb}\sqrt{f_{cw}}) + 2.75\times10^{-3}(f_{ystb}) - 2.14(S_{sc})$$

$$\mu_u = \frac{d_u}{d_y} = 54.57 - 7.7(\rho_{tb}) + 23.33(\rho_{vtb}) - 403.2(d_c) + 1388.5(A_c) - 0.09(f_y) + 1.23\times10^{-3}\left(\frac{12E_{cf}I_c}{h_c^3}\right) + 582.71(A_o) - 64.71(A_{ov}) - 432.04(t_p) + 27.82\left(\frac{L_{tb}}{n.L_{pe}}\right) + 0.047(f_{ya}) - 54(A_{ca}f_{ya})$$

where

A_w = Horizontal cross sectional area of the infill wall and columns (m^2)
A_{cg} = Gross cross sectional area of each column (m^2)
A_c = Effective area of each column (m^2)
A_o = Horizontal cross sectional area of infill wall's opening (m^2)
A_{ov} = Vertical cross sectional area of infill wall's opening (m^2)
A_{ca} = Total cross sectional area of connecting anchors on each column (m^2)
A_{stb} = Total area of rebars crossing the interface between shear wall and top beam of frame (for monolithic shear wall only, m^2)
A_{tb} = Effective area of top beam (m^2)
A_{bb} = Effective area of bottom beam (m^2)
d_c = Column effective depth (m)
d_u = Lateral displacement at ultimate load P_u (m)
d_y = Lateral displacement at yield (m)
E_{cf} = Young's Modulus of steel reinforcement (MPa)
f_{cw} = Concrete compressive strength of infill wall (MPa)
f_{cf} = Concrete compressive strength of frame (MPa)
f_y = Material yield strength of frame reinforcement (MPa)
f_{ya} = Material yield strength of anchors (MPa)
f_{yw} = Yield strength of infill wall's reinforcement (MPa)
f_{ystb} = Material yield strength of rebars crossing the interface between shear wall and top beam of frame in monolithic frame-shear wall construction (MPa)
h_c = story height (m)
I_c = Moment of inertia of frame's horizontal cross section (only two columns, excluding wall) (m^4)
I_w = Moment of inertia of horizontal cross section of columns and infill wall (m^4)
L_{tb} = Top beam span length (m)
L_{pc} = Length of each precast panel used as infill wall (m)
n = Number of precast panels used in infilling the frame
P_u = Ultimate in-plane lateral load applied at center of top beam (MN)
P_{xc} = Axial force in each column (MN)
S_{atb} = Spacing of anchors on top beam (m)
S_{sc} = Spacing of connecting rebars on the interface between shear wall and column in monolithic frame-wall construction (m)
S_{sbb} = Spacing of rebars on the interface between shear wall and bottom beam of frame (m)
t_w = Thickness of infill wall (m)
t_p = Thickness of precast panels used as infill wall (m)
ρ_{tb} = Flexural reinforcement ratio of top beam (%)
ρ_{bb} = Flexural reinforcement ratio of bottom beam (%)
ρ_c = Flexural reinforcement ratio of each column (%)
ρ_{vtb} = Shear reinforcement ratio of top beam (%)
μ_u = ductility factor (d_u/d_y)

4.2 VALIDATION OF EMPIRICAL FORMULAS FOR P_u/A_w, d_u/d_y, and μ_u

For validation, the above empirical formulas were used to estimate ultimate lateral shear strength (P_u/A_w), story drift ratio at ultimate load (d_u/h_c), and ductility factor μ_u (d_u/d_y) of the fifty-four test frames used in this study. The estimations were plotted against the experimental results in the form of scatter plots, as shown in Figures 4.2, 4.4, and 4.6. Ideally, all points on these scatter plots should be on the 45 degree line as shown on the plots, which would mean the estimations were extremely accurate (within the limit of the fifty-four tests). However, this is impossible to achieve, especially considering the statistical nature of the empirical formulas. Thus, error plots, as shown in Figures 4.3, 4.5, and 4.7, were used to facilitate an assessment of the accuracy of the estimations.

From Figures 4.2 to 4.7, important ranges for ultimate shear strength, ultimate story drift, and ductility factor of existing frames, monolithic shear walls, frames strengthened by CIP infill walls and by multiple precast wall panels, are revealed. These ranges confirmed the expected trend observed by many individual experimental programs. In this sense, the derived empirical formulas prove to be valid. The following points are considered noteworthy:

- The majority of the estimates for frame ultimate shear strength (P_u/A_w) fall within the 20 percent error limit. Estimates for existing frames and frames strengthened by precast infill walls appear to be less accurate than for the cases of CIP infill walls and monolithic shear walls. This is probably due to the limited number of tests for existing frames (5 tests) and precast infill walls (8 tests) included in the data base.

- In terms of lateral shear strength, existing frames naturally have the lowest strength with the average shear strength of 1.0 MPa. Strengthening the frames using precast concrete panels appears to increase the infilled frame's shear capacity only marginally, as indicated in the scatter plot (to an average shear strength of 1.3 MPa). Infilling the frames by CIP infill walls appears to significantly increase the frame shear capacity (to an average shear strength of 3 MPa), approaching that of monolithic shear walls (average shear strength of 3.5 MPa).

- For all types of frames considered, the majority of the frames have lateral ultimate shear strength which falls within the range of 1 to 4 MPa.

- In terms of story drift ratio at ultimate load, CIP infilled frames appear to have the smallest story drift ratio (almost all have less than 1 percent). Monolithic shear walls appear to be next higher in story drift ratio, then precast infilled frames, and lastly, existing frames appear to have the largest story drift ratio.

- The majority of estimates for story drift ratio using the derived expression fall within the bounds of 25 percent error, according to the error plot.

- All types of frames considered, the majority of the frames have story drift ratios which fall within the range of 0.5 to 2.5 percent.

- The majority of the frames have a ductility factor (defined as the ratio between story drift at ultimate load d_u and story drift at yield d_y) in the range of 5 to 30. The constructions appearing to have the smallest ductility factor are the monolithic shear walls and the CIP infill walls. However, the estimations for ductility factor appear to have larger error than those for ultimate shear strength and ultimate story drift ratio, with bounds of error of up to 50 percent.

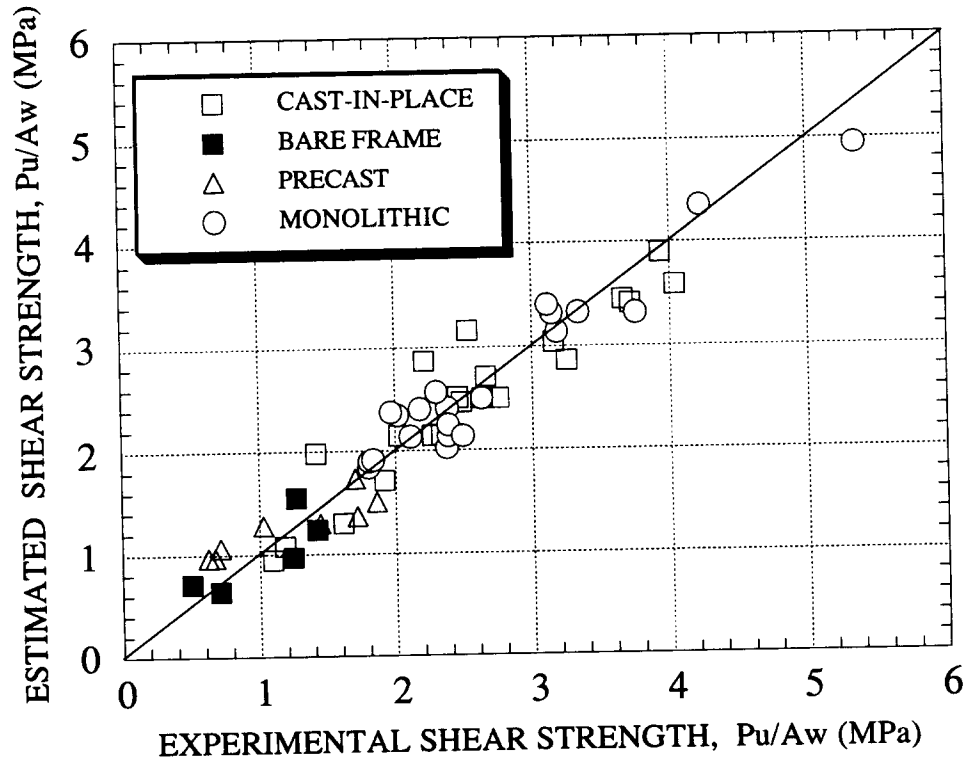

Figure 4.2 Predicted vs. Experimental Shear Strength of Frames

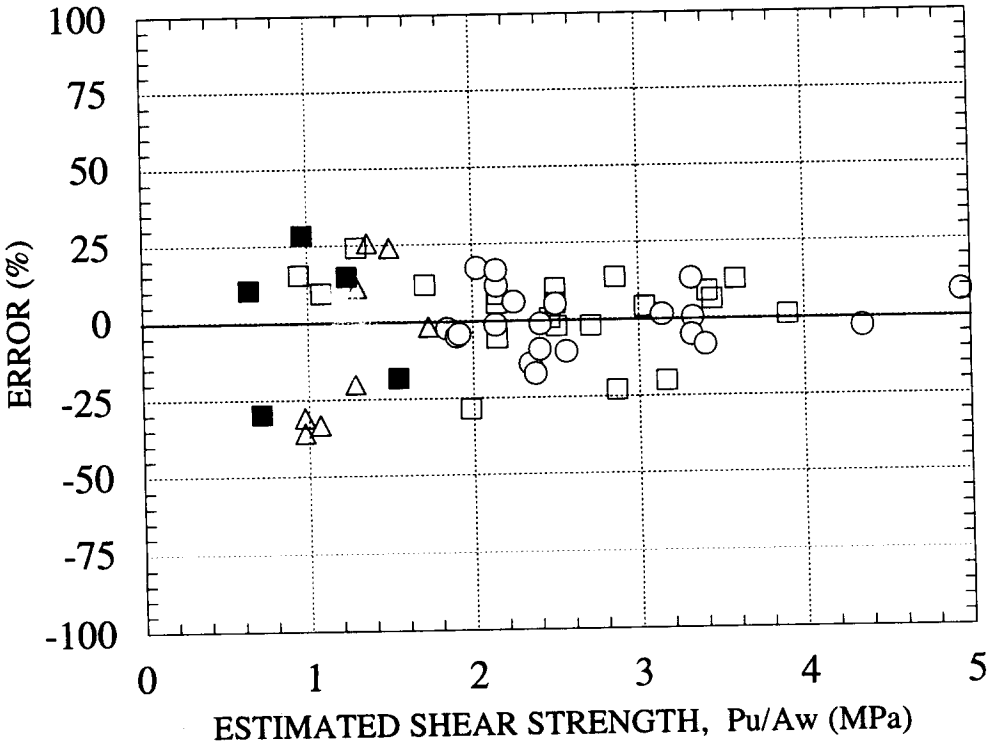

Figure 4.3 Error in Shear Strength Predictions

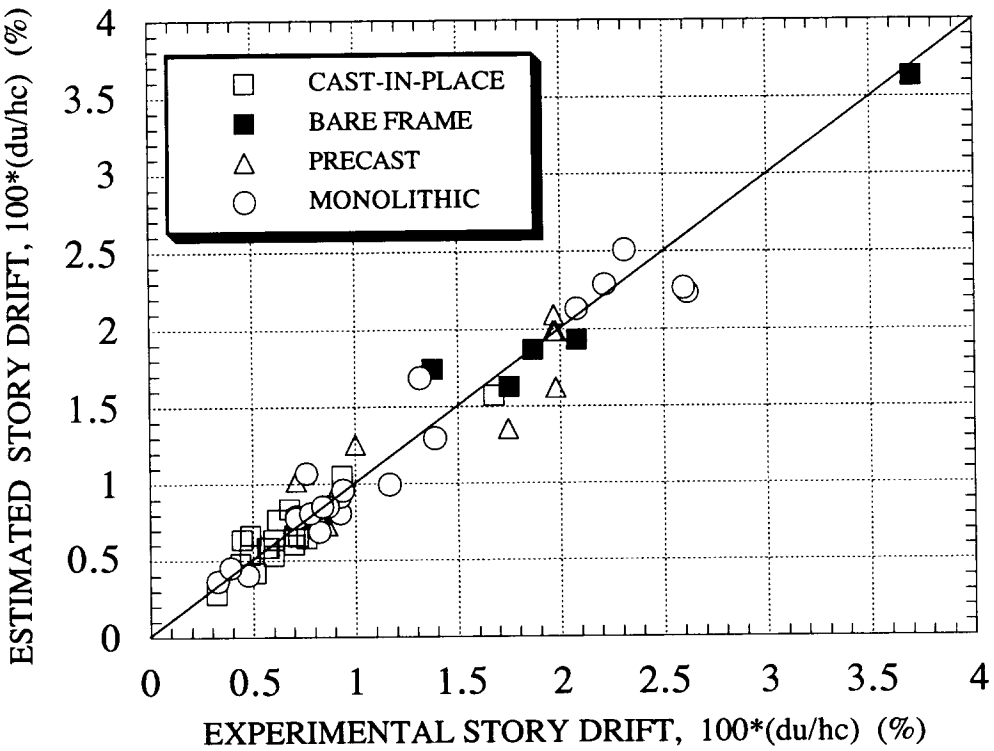

Figure 4.4 Predicted vs. Experimental Story Drift Ratio

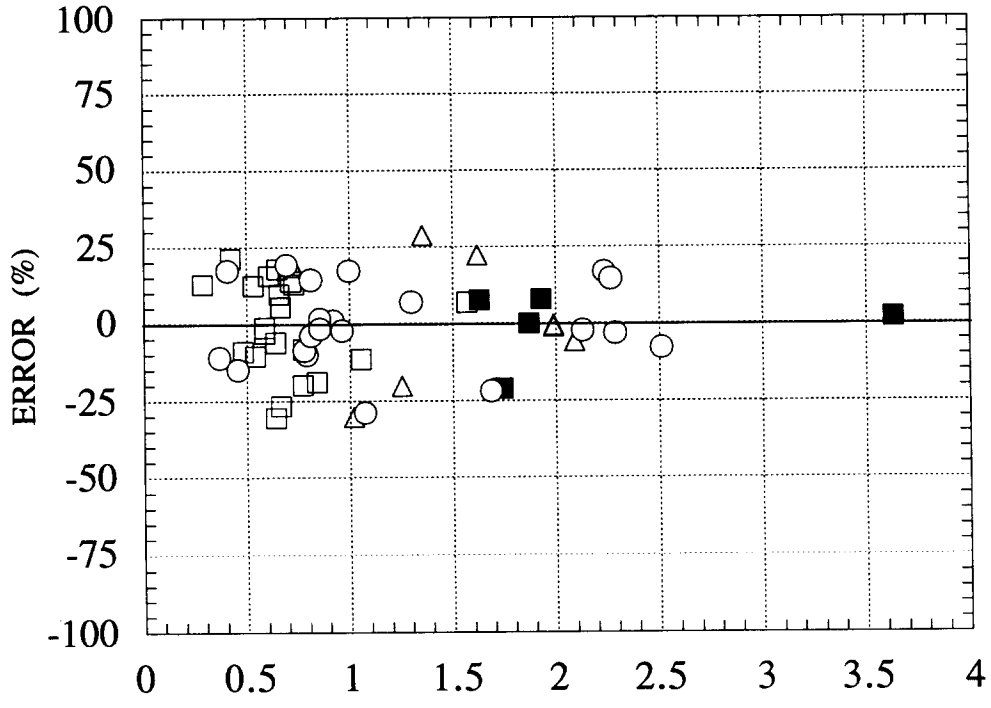

Figure 4.5 Error in Story Drift Ratio Predictions

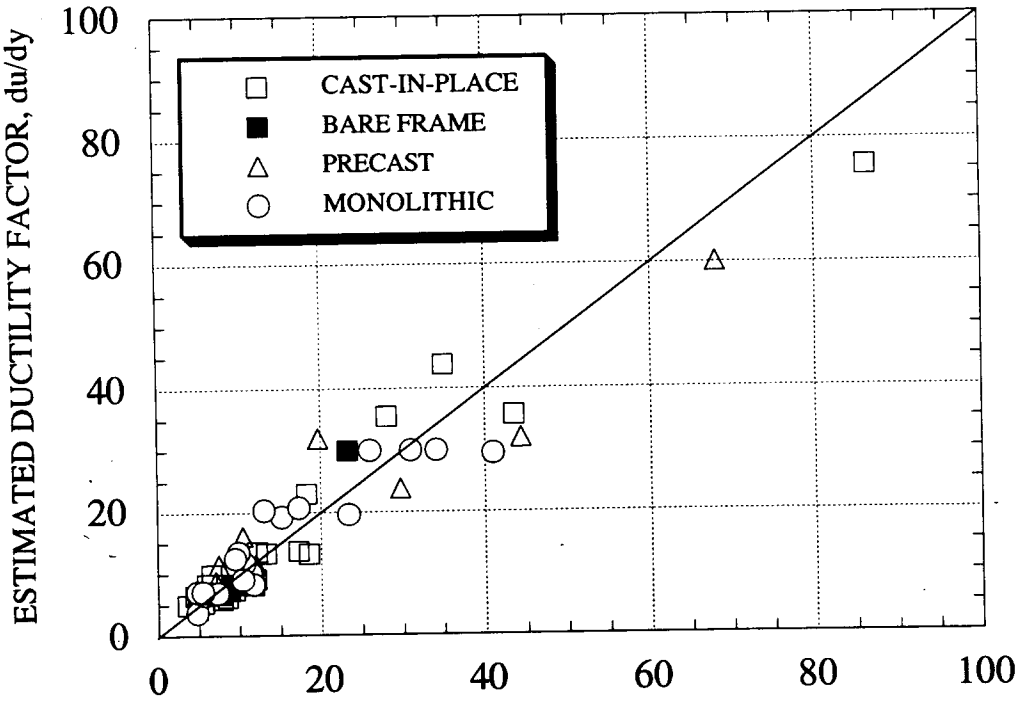

Figure 4.6 Predicted vs. Experimental Ductility Factor

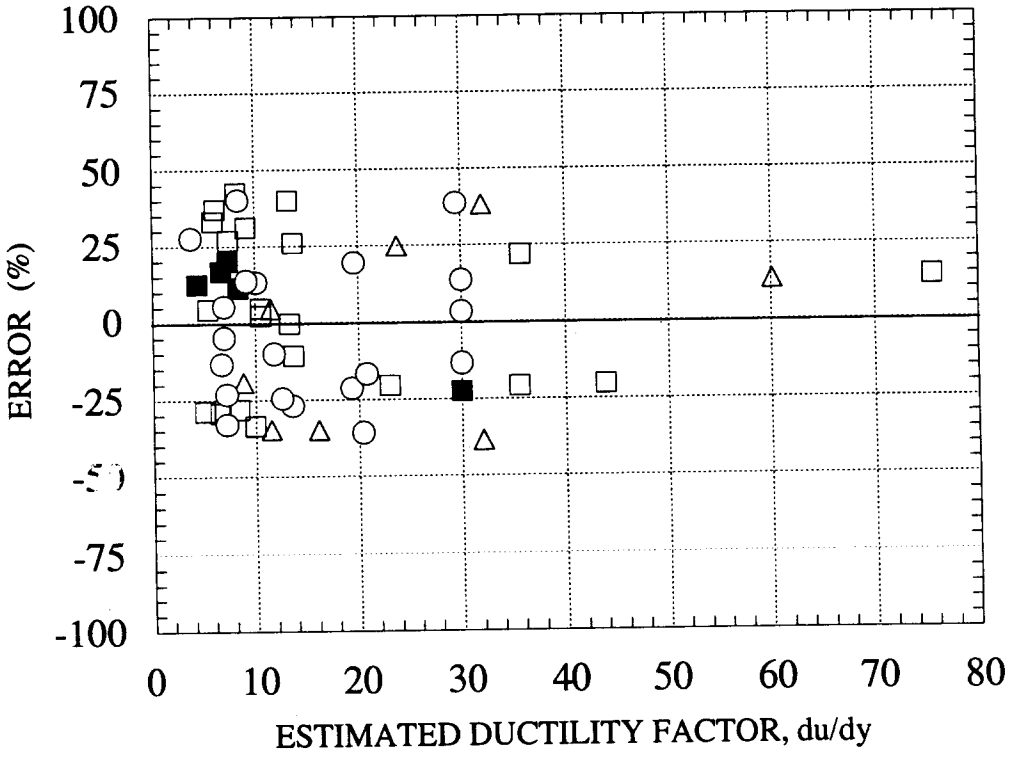

Figure 4.7 Error in Ductility Factor Predictions

Chapter 5

TOWARDS DESIGN GUIDELINES: SUMMARY OF OBSERVATIONS FROM EXPERIMENTAL PROGRAMS

5.1 GENERAL

As discussed earlier, the objective of this NIST's research program is to develop guidelines for the design of infill walls to strengthen existing LRC frames. At this stage of the research, two computational methods have been developed and are recommended as design tools for use in evaluating seismic performance of existing frames and frames strengthened by two variations of the infill wall technique (infilling by cast-in-place RC walls and infilling by precast RC panels). The first computational method involves the use of hysteresis failure models, developed earlier in the course of this project (Phan et al., 1993), and the platform program IDARC. The second method, described in this report, represents a simplified, empirical means to calculate the three critical parameters for the design of infilled frames, namely the ultimate shear strength, the story drift ratio, and the ductility factor. Further, review of published experimental programs also revealed some important details for the design of infill walls which have resulted in successful or improved seismic performance of the strengthened frames. These design details are listed below as potential for future design guidelines and are subjected to future sensitivity study for validation. Recommendations for design guidelines will be made once the sensitivity study is completed.

5.2 POTENTIAL DESIGN GUIDELINES FOR STRENGTHENING WITH INFILL WALLS

5.2.1 **Design of Infill Walls**

The following experimental details were observed to be critical for successful design of infill walls and are subjected to future validation through a sensitivity study:

- Infill wall thickness, of both CIP and precast infill walls, should be not less than 2/5 the thickness of the bounding column or the top beam of the frame, whichever is smaller, and should be not greater than the thickness of the top beam.

- Infill wall, either CIP, precast, or shotcrete, should be constructed using concrete with normal range of compressive strength (14 - 50 MPa). The design compressive strength of the infill wall should be compatible with that of the existing frame.

- Either mechanical wedge anchors or epoxied dowels can be used to connect CIP infill walls to the existing frame. For precast infill walls, only epoxy grouted dowels are recommended. The connectors should be placed, at a minimum, on the interface between the infill walls and top and bottom beams, in predrilled holes on the inner surface of the frame to be strengthened. The connectors should be located as close to the center line of the concrete infill wall as possible so as to minimize the eccentricity of the transfer shear force with respect to the center line of the infill walls.

- The ratio of the total cross sectional area of the connectors and the area of the infill walls on the wall/frame interface should be not less than 0.8 percent.

- The connector size can be selected based on the above required area of connectors and a connector spacing of not less than 7 D_b and not greater than 30 cm. D_b is the outside diameter of the connectors.

- Where more than one line of connectors is required on the infill wall/frame interface due to the required total area of connectors given above, the distance between the connector lines should be not less than 5 D_b.

- Embedment depth of connectors should be, in principle, not less than 5 D_b or the thickness of the concrete cover, whichever is greater.

- The infill walls should be reinforced in flexure both horizontally and vertically with a reinforcing ratio of not less than 0.75 percent. Shear reinforcement of 0.25 to 1.0 percent should be provided for confinement of concrete in the infill walls.

5.2.2 Expected Lateral Strength, Story Drift Ratio, and Ductility Factor

Review of existing experimental data has shown the following values can be expected for shear strength, story drift ratio, and ductility factor:

- The expected range of lateral shear strength of a unit one-story one-bay LRC frame, normalized with respect to the plan area of the frame and the infill wall (where A_w equals the plan area of the two bounding columns and the infill wall), is as follows:

  - 0.65 to 1.6 MPa for existing, unstrengthened frames†.
  - 0.9 to 1.7 MPa for frames strengthened using precast concrete panels†.
  - 1.0 to 3.9 MPa for frames strengthened by CIP infill walls†.
  - 1.8 to 4.9 MPa for monolithic shear walls†.

  †It should be noted that these average shear strengths are expressed in terms of ultimate shear stress at the base of the frames (force P_u divided by plan area A_w). Since the plan area of the bare frame consists of the area of the two bounding columns only, and the plan areas of the latter three constructions include the plan area of the infill walls, the relative differences between the strengths of the latter three frames and the bare frame listed above do not appear to be as large as when the lateral forces P_u are compared.

- The expected range of story drift ratio at ultimate load (d_u/H_c) of a unit one-bay one-story RC frames is as follows:

  - 0.3 to 1.6% for CIP infilled frames.
  - 0.4 to 2.5% for monolithic shear walls.
  - 0.7 to 2.1% for precast infilled frames.
  - 1.6 to 3.6% for bare frames.

- It is more difficult to discern the ductility factor of each type of frame constructions. In general, the majority of frame constructions have a ductility factor (defined as the ratio between story drift at ultimate load d_u and story drift at yield d_y) in the range of 5 to 30. The range of ductility factor of each type of RC frame is as follows: